ELSEVIER

Image and Vision Computing 18 (1999) 39–48

image AND vision COMPUTING

www.elsevier.com/locate/imavis

Cephalogram analysis applying template matching and fuzzy logic

S. Sanei PhD*, P. Sanaei MSc, M. Zahabsaniei DDS

Electronic and Communication Engineering Department, Singapore Polytechnic, 500 Dover Road, Singapore 139651, Singapore

Received 10 August 1998; received in revised form 10 June 1999; accepted 25 June 1999

Abstract

Cephalogram analysis has an important role in diagnosis, treatment and surgery of the skull and jaw. This field of science is mostly used by orthodontists. High speed and accuracy in automatic detection and geometrical evaluation and description of landmarks is widely demanded. An iterative self-organized data analysis technique using a combination of statistical pattern recognition and fuzzy logic-based decision making has been proposed as an efficient technique for detection of craniofacial landmarks. A large number of cephalograms has been considered in order to testify the performance of the system against different quality images. The images are primarily processed in order to enhance the regions of soft and hard tissues separately. Then for each landmark, different template matching plus fuzzy logic approach has been followed. Final landmarks are selected from a number of detected points by applying another fuzzy decision making criterion. The procedure is superior to the previous techniques for which either low accuracy has been reported or high quality images have been taken into consideration.

Keywords: Cephalogram; Template matching; Fuzzy logic

1. Introduction

Cephalograms are lateral skull (craniofacial) X-radiographs. Cephalometric radiography was introduced to orthodontics in 1930 by Brodic, Boidbent and Hofraeh. Since 1960 it has been widely used by specialists. These images are widely used in orthodontics and jaw surgery [1,2]. Geometrical evaluation and description of a set of points or features (landmarks) in soft and hard tissue projections in these images provide sufficient clinical information. Locating dominant landmarks and their relative geometrical identifiers are the major objectives in cephalometry. As plane X-ray images are normally blurred, even now most orthodontic pathologists use their eye to mark the points and manually measure the geometrical parameters such as size of the links between each of two points and the angle between each pair of links. Because the manual method is a very time consuming process, automatic cephalometry has become of great importance. However, manual techniques may be replaced by computerized methods if sufficient accuracy can be achieved. In that case, the degree of accuracy is dependent on the applied algorithm. Recently reported methods in computerized cephalometry either suffer from inaccurate estimation of the desired features or consider only special good quality images [3]. As most of the proposed algorithms are based on the extracted boundary information, they usually fail in highly accurate detection of the features from low contrast X-ray images. Application of a global data-based system can only with difficulty be adapted to various data, particularly to infant cephalograms. In the methods where morphological operators are used, most of the targets are detected with low accuracy due to the same reason.

Pattern matching is a routine procedure to underline the similarities between the patterns. However, definition of feature-oriented synthetic patterns is an important task. In this work, application of the method leads to arrangement of a number of clusters for each landmark. With pre-knowledge of approximate location, size of the skull and location of the features relative to each other, an approximate reasoning following a rule-based Fuzzy Logic (FL) [4] has been applied to select the desired cluster. Moreover, for justification of the overall geometrical location of the landmarks another fuzzy criterion further enhances the accuracy. Unlike crisp, fuzzy logic exploits all existing information considering the possibilities.

In the following sections we describe the concepts of cephalometry, enhancement of images, detection of the clusters for each landmark, application of FL to the clusters to detect the landmarks and justification of accurately detected landmarks using another FL criterion.

* Corresponding author. Tel. + 65-7721380; fax: + 65-7721974.
E-mail address: ssanei@sp.edu.sg (S. Sanei PhD)

0262-8856/99/$ - see front matter
PII: S0262-8856(99)00013-X

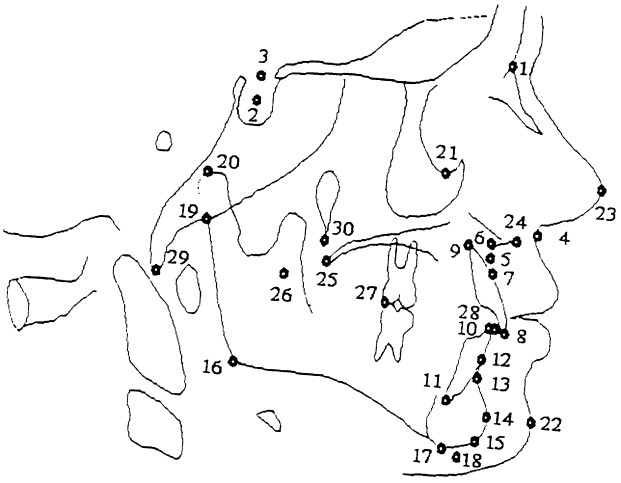

Fig. 1. Lateral skull profile.

2. Craniofacial pattern

Most orthopedic abnormalities in the skull, especially malocclusions, may be diagnosed by considering the location and geometrical description of about 30 landmarks in the lateral skull profile. The landmarks are detected and geometrically evaluated in order to diagnose the abnormalities and monitor the treatment. These features are depicted in the profile of Fig. 1. The points are Nasion, Sella Turcica, Mid point of entrance to Sella, Subnasal, Subspinal point A, AP max, Prosthion, Superior Incisor Apical 1, Inferior Incisor, Apical 2, Infradental, Supramental point B, Pogonion, Gnathion, Gonion, Menton, AP man, Articular, Condylion, Orbital, Soft tissue Pogonion, Tip of the nose, Anterior nasal spine, Posterior nasal spine, S point, A_{pocc}, P_{poss}, Basion and Ptm, respectively. 13 Landmarks are widely used in diagnosis of different classes of malocclusions. These features are Nasion, Sella Turcica, Tip of the nose, Subnasal, Point A, Point B, Menton, Gonion, Superior Incisor, Gnathion, Maxillary plane, Mandibular plane and Occlusal plane [1,2]. Malocclusion is basically due to improper positions of Mandibular and maxillary planes with respect to each other. Fig. 2 shows two known classes of malocclusion called class 1 and class 2.

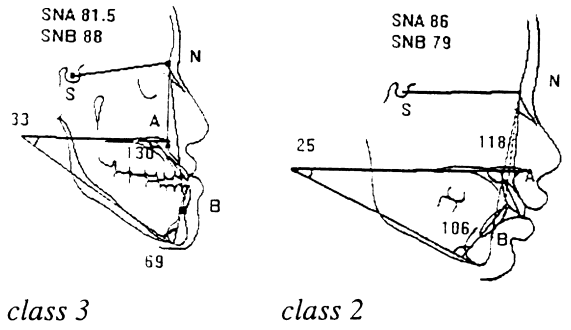

Fig. 2. The two classes of malocclusion.

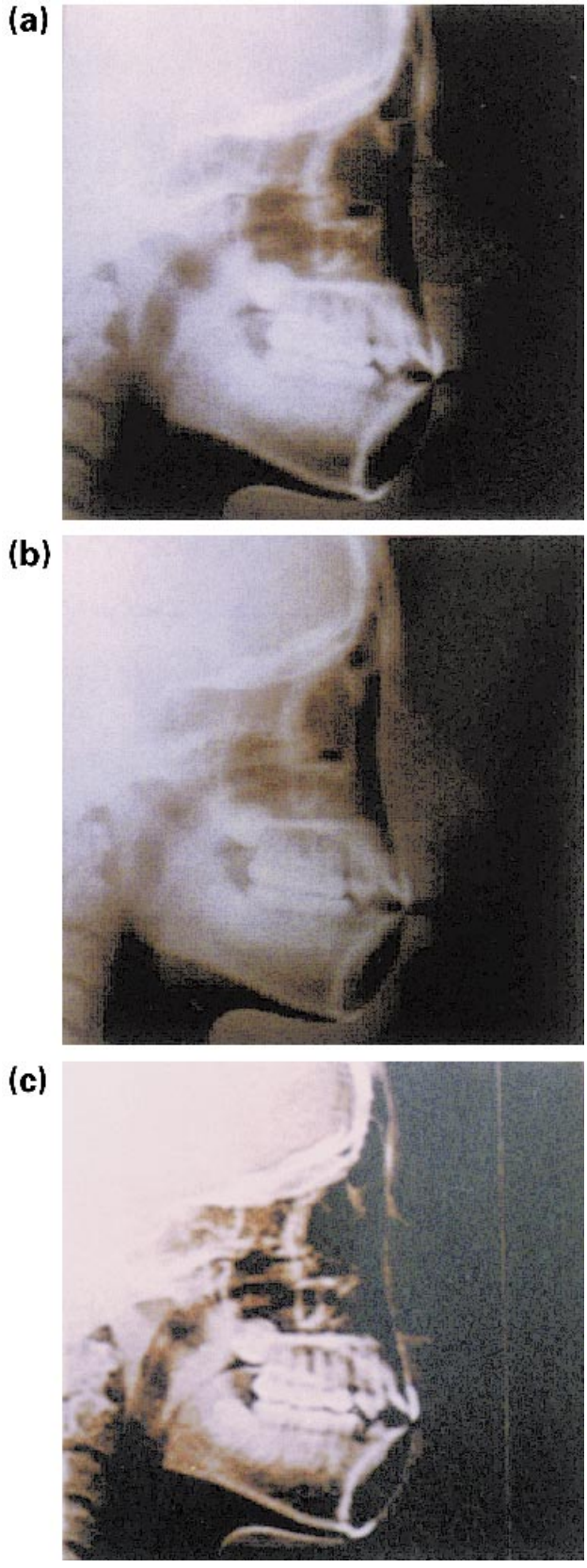

Fig. 3. Original and enhanced images: (a) original; (b) soft tissue enhanced; and (c) hard tissue enhanced.

3. Pre-processing of cephalograms

In order to process the images using a computer, they are digitized to 256 grey level. To decrease computation cost, only 256×256 size images are considered. Certainly for higher resolution images, the accuracy of processing would be further enhanced. Vatcom C compiler has been used for our programming. The software enables fast access to the subroutines and the images. In the first step the images are restored from noise and the desired features are enhanced in order to facilitate the recognition process. As the processing is mostly based on local data statistics, proper segmentation of the histogram into two parts clearly discriminates between soft and hard lesions in the image. Application of a side-information median filter [5] together with two-dimensional band-pass Gaussian filtering ($\mu = 35$, $\sigma = 30$) effectively highlights the edges while reducing the high spatial frequency noise. Fig. 3 illustrates the original image together with the images of enhanced soft and hard tissues.

To enable accurate template matching in the vicinity of the features, the edges should be enhanced and detected. As still X-ray images are naturally blurred, popular edge detection procedures based on gradient measurement such as Sobel fail in the efficient extraction of the edges. The method applied here fits two lines to the adjacent segments of each row or column of the image. Assuming the lines to be y_1 and y_2 as

$$y_1 = a_1 x + b_1 \quad (1)$$

and

$$y_2 = a_2 x + b_2 \quad (2)$$

Empirical definition of triangular shape membership functions [4] leads to simple fuzzy decision making for detection of the edges:

> if a_1 and a_2 are different by a threshold or b_1 and b_2 are different when a_1 and a_2 are almost equal then an edge is detected.

Fuzzy calculation has been utilised in order to manipulate linguistic and qualitative variables as well as numerical and quantitative parameters. FL is a powerful tool in manipulation of uncertainty in the data [6].

4. Detection of landmarks

Two steps are followed in the method based on the Automatic Target Recognition idea; search for possible clusters and selection of each feature from the dominant cluster mainly based on Maximum-correlation criterion [7]. Based on primary knowledge about the organ, its approximate location, type of tissue (hard or soft), and global and local image statistics, a search zone is primarily determined for each landmark. Thus by considering smaller regions the computation cost decreases and the processor is simplified. Definition of a proper template is also an important task in clustering based on pattern matching procedure. In the following sections a brief explanation for detection of each landmark is given.

4.1. Tip of the nose

Looking at the right side of the face, the tip of the nose is usually (not always) the point in the most extreme right of lateral skull image. General and statistical information in soft-tissue-enhanced-image is exploited in definition of a 16×16 rectangular template, N_1, defined as

$$N_1 = \begin{bmatrix} 1&1&1&1&1&1&1&1&0&0&0&0&0&0&0&0\\ 1&1&1&1&1&1&1&1&0&0&0&0&0&0&0&0\\ 1&1&1&1&1&1&1&1&0&0&0&0&0&0&0&0\\ 1&1&1&1&1&1&1&1&0&0&0&0&0&0&0&0\\ 1&1&1&1&1&1&1&1&0&0&0&0&0&0&0&0\\ 1&1&1&1&1&1&1&1&0&0&0&0&0&0&0&0\\ 1&1&1&1&1&1&1&1&0&0&0&0&0&0&0&0\\ 1&1&1&1&1&1&1&1&0&0&0&0&0&0&0&0\\ 1&1&1&1&1&1&1&1&0&0&0&0&0&0&0&0\\ 1&1&1&1&1&1&1&1&0&0&0&0&0&0&0&0\\ 1&1&1&1&1&1&1&1&0&0&0&0&0&0&0&0\\ 1&1&1&1&1&1&1&1&0&0&0&0&0&0&0&0\\ 1&1&1&1&1&1&1&1&0&0&0&0&0&0&0&0\\ 1&1&1&1&1&1&1&1&0&0&0&0&0&0&0&0\\ 1&1&1&1&1&1&1&1&0&0&0&0&0&0&0&0\\ 1&1&1&1&1&1&1&1&0&0&0&0&0&0&0&0 \end{bmatrix}$$

and identification of the corresponding clusters. The clusters include the points around the tip of the nose, the points around tip of the lower lip and those around upper lip. Also due to our primary information about the approximate location, the search area is limited to x_{85-255} and y_{64-192} within the 256×256 image. Cross-correlation of N_1 and blocks of similar size centred at jth pixel of the ith column of the search region, $\rho(i,j)$, where

$$\rho_i(j) = \frac{\sum_{l=-7}^{8} \sum_{m=-7}^{8} N_1(l+7, m+7) X(l+7, m+7)}{\sum_{l=0}^{15} \sum_{m=0}^{15} N_1^2(l,m) \sum_{l=-7}^{8} \sum_{m=-7}^{8} X^2(i+l, j+m)} \quad (3)$$

gives the degree of similarities between the template and the image sub-block. ρ is evaluated for each value of i up to a maximum, and variance of ρ is calculated in order to define a suitable threshold value each time:

$$\rho_T = \frac{1}{3}(\rho_{\max} - \rho_{\mathrm{mean}}) + \rho_{\mathrm{mean}} \quad (4)$$

The search continues until either it reaches the end of the region or a considerable change in variance of ρ, σ_ρ^2 occurs

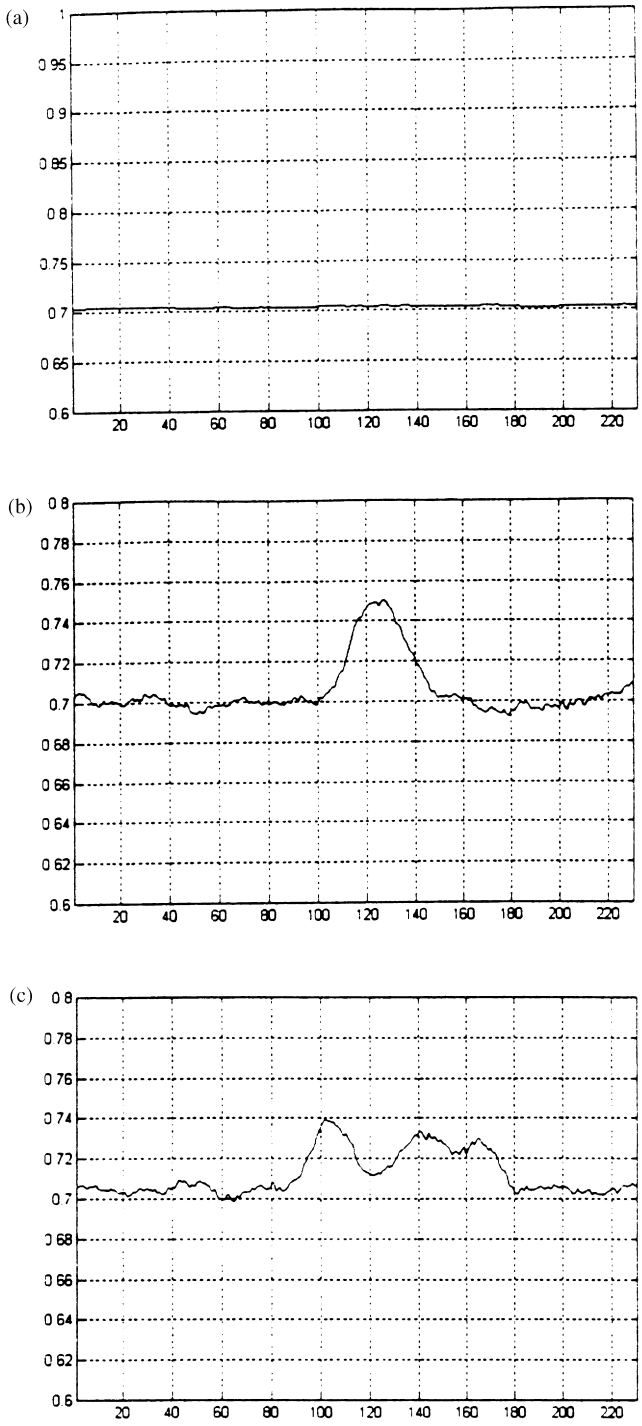

Fig. 4. ρ for: (a) background noise; (b) cross-section of tip of the nose region; and (c) cross-section of the lips region.

(Fig. 4). The latter case shows that we have reached the hard tissue. Now, a number of clusters including the detected points are assumed as an observation to the fuzzy decision making system. The reasoning will be based on the following implications:

1. the number of class members is “not low”;
2. the class is “close to the right edge” of the image;
3. there are two other classes “lower left” and “almost in line” with this class (belong to the tip of the lips).

Considering simple trapezoidal membership functions for the linguistic parameters *not low*, *close* and *lower left* and *almost in line* based on empirical measurements, such as those depicted in Fig. 5, simple reasoning leads to selection of the required cluster.

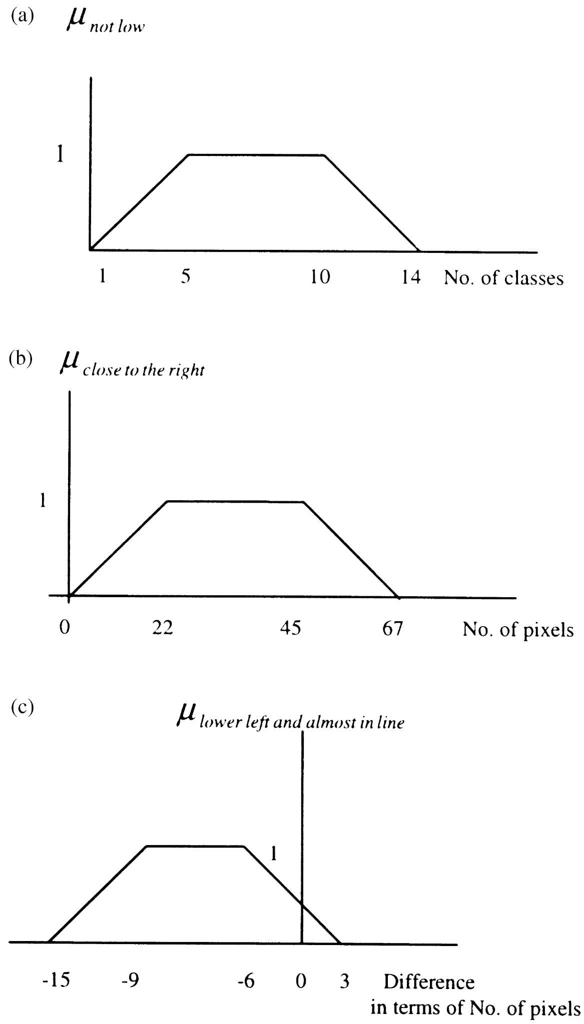

Fig. 5. Membership functions for: (a) not low; (b) close to the right edge; (c) lower left and almost in line.

A similar search is then carried out in the vicinity of the selected cluster with a radius of 20 using a similar but smaller size 6×6 template. Following the above procedure, the tip of the nose will be detected with 100% accuracy. Moreover, the tip of the lips also may be marked in another stage that may be exploited in recognition of the other landmarks.

4.2. Subnasal

The coordinates of the tip of the nose in the cephalogram are used as primary knowledge in detection of Subnasal. The search area is a region of size 40×40 for which the tip of the nose is located in the top left corner. The image sub-block, X, is already enhanced using histogram equalization [8,9] and low-pass filtered using 3×3 averaging operator. A bilevel image sub-block is achieved by using a threshold based on identification of histogram global minima. In such an image soft tissue and background are well separated. Tip of the nose and Subnasal are located on the boundary line for which $X(i,j) - X(i-1,j) > 0$. If $f(i)$ represents the boundary, absolute minima for $f(i)$ will be equivalent to the subnasal point. Fig. 6 illustrates the concept.

4.3. Superior Incisor

Anatomical and physiological characteristics of the head and neck together with already obtained information are exploited in detection of the Superior Incisor. Soft tissue and background noise are already eliminated by using an adaptive histogram-based threshold. The closest candidates are selected via cross-correlation of the sub-blocks in the vicinity of the landmark, and a 15×15 template N_2 similar to N_1. The dominant class will then be selected based on the following conditions:

1. the cluster is "close" to the right edge;
2. the cluster is "slightly below" subnasal point;
3. the cross-correlation is maximum.

Trapezoidal membership functions for close and *slightly below* are empirically achieved by taking a number of exemplars into considerations. Fig. 7 illustrates the above functions. Superior Incisor is a point in the dominant cluster. A search will be conducted again over a window of size 40×40 in the vicinity of the cluster, using the 15×15 template, N_3, defined as

$$N_3 = \begin{bmatrix} 1&1&1&1&1&1&1&1&0&0&0&0&0&0&0 \\ 1&1&1&1&1&1&1&1&0&0&0&0&0&0&0 \\ 1&1&1&1&1&1&1&1&0&0&0&0&0&0&0 \\ 0&1&1&1&1&1&1&1&0&0&0&0&0&0&0 \\ 0&0&1&1&1&1&1&1&0&0&0&0&0&0&0 \\ 0&0&0&1&1&1&1&1&0&0&0&0&0&0&0 \\ 0&0&0&0&1&1&1&1&0&0&0&0&0&0&0 \\ 0&0&0&0&0&0&0&0&0&0&0&0&0&0&0 \\ 0&0&0&0&0&0&0&0&0&0&0&0&0&0&0 \\ 0&0&0&0&0&0&0&0&0&0&0&0&0&0&0 \\ 0&0&0&0&0&0&0&0&0&0&0&0&0&0&0 \\ 0&0&0&0&0&0&0&0&0&0&0&0&0&0&0 \\ 0&0&0&0&0&0&0&0&0&0&0&0&0&0&0 \\ 0&0&0&0&0&0&0&0&0&0&0&0&0&0&0 \\ 0&0&0&0&0&0&0&0&0&0&0&0&0&0&0 \end{bmatrix}$$

Finally, the point for which the cross-correlation function (similarity) is maximum, is Superior Incisor.

4.4. Maxillary and occlusal planes

The relative position of maxillary and mandibular planes determines different occlusal classes. Class 1 corresponds to normal occlusion. Classes 2 and 3 represent malocclusion (Fig. 2). The margin points are detected by template

matching. The planes are nicely recognized by tracking the corresponding contours in proper directions. The search is started from Superior Incisor. The directions are cleverly detected by LSF-based [6] minimisation of Euclidean distances between the selected points and the representative point of each class. For this application, the new member of each class is considered as its representative. Cross-correlation of the templates N_4 and N_5 defined as

$$N_4 = \begin{bmatrix} -1 & -1 & -1 & -1 & -1 & -1 & -1 & -1 & -1 & -1 & -1 & -1 & -1 & -1 & -1 \\ -1 & -1 & -1 & -1 & -1 & -1 & -1 & -1 & -1 & -1 & -1 & -1 & -1 & -1 & -1 \\ -1 & -1 & -1 & -1 & -1 & -1 & -1 & -1 & -1 & -1 & -1 & -1 & -1 & -1 & -1 \\ -1 & -1 & -1 & -1 & -1 & -1 & -1 & -1 & -1 & -1 & -1 & -1 & -1 & -1 & -1 \\ -1 & -1 & -1 & -1 & -1 & -1 & -1 & -1 & -1 & -1 & -1 & -1 & -1 & -1 & -1 \\ -1 & -1 & -1 & -1 & -1 & -1 & -1 & -1 & -1 & -1 & -1 & -1 & -1 & -1 & -1 \\ -1 & -1 & -1 & -1 & -1 & -1 & -1 & -1 & -1 & -1 & -1 & -1 & -1 & -1 & -1 \\ 1 & 1 & 1 & 1 & 1 & 1 & 1 & 1 & 1 & 1 & 1 & 1 & 1 & 1 & 1 \\ 1 & 1 & 1 & 1 & 1 & 1 & 1 & 1 & 1 & 1 & 1 & 1 & 1 & 1 & 1 \\ 1 & 1 & 1 & 1 & 1 & 1 & 1 & 1 & 1 & 1 & 1 & 1 & 1 & 1 & 1 \\ 1 & 1 & 1 & 1 & 1 & 1 & 1 & 1 & 1 & 1 & 1 & 1 & 1 & 1 & 1 \\ 1 & 1 & 1 & 1 & 1 & 1 & 1 & 1 & 1 & 1 & 1 & 1 & 1 & 1 & 1 \\ 1 & 1 & 1 & 1 & 1 & 1 & 1 & 1 & 1 & 1 & 1 & 1 & 1 & 1 & 1 \\ 1 & 1 & 1 & 1 & 1 & 1 & 1 & 1 & 1 & 1 & 1 & 1 & 1 & 1 & 1 \\ 1 & 1 & 1 & 1 & 1 & 1 & 1 & 1 & 1 & 1 & 1 & 1 & 1 & 1 & 1 \end{bmatrix}$$

$$N_5 = \begin{bmatrix} 1 & 1 & 1 & 1 & 1 & 1 & 1 & 1 & 1 & 1 & 1 & 1 & 1 & 1 & 1 \\ 1 & 1 & 1 & 1 & 1 & 1 & 1 & 1 & 1 & 1 & 1 & 1 & 1 & 1 & 1 \\ 1 & 1 & 1 & 1 & 1 & 1 & 1 & 1 & 1 & 1 & 1 & 1 & 1 & 1 & 1 \\ 1 & 1 & 1 & 1 & 1 & 1 & 1 & 1 & 1 & 1 & 1 & 1 & 1 & 1 & 1 \\ 1 & 1 & 1 & 1 & 1 & 1 & 1 & 1 & 1 & 1 & 1 & 1 & 1 & 1 & 1 \\ -1 & -1 & -1 & -1 & -1 & -1 & -1 & -1 & -1 & -1 & -1 & -1 & -1 & -1 & -1 \\ -1 & -1 & -1 & -1 & -1 & -1 & -1 & -1 & -1 & -1 & -1 & -1 & -1 & -1 & -1 \\ -1 & -1 & -1 & -1 & -1 & -1 & -1 & -1 & -1 & -1 & -1 & -1 & -1 & -1 & -1 \\ -1 & -1 & -1 & -1 & -1 & -1 & -1 & -1 & -1 & -1 & -1 & -1 & -1 & -1 & -1 \\ -1 & -1 & -1 & -1 & -1 & -1 & -1 & -1 & -1 & -1 & -1 & -1 & -1 & -1 & -1 \\ & 1 & 1 & 1 & 1 & 1 & 1 & 1 & 1 & 1 & 1 & 1 & 1 & 1 & 1 \\ 1 & 1 & 1 & 1 & 1 & 1 & 1 & 1 & 1 & 1 & 1 & 1 & 1 & 1 & 1 \\ 1 & 1 & 1 & 1 & 1 & 1 & 1 & 1 & 1 & 1 & 1 & 1 & 1 & 1 & 1 \\ 1 & 1 & 1 & 1 & 1 & 1 & 1 & 1 & 1 & 1 & 1 & 1 & 1 & 1 & 1 \\ 1 & 1 & 1 & 1 & 1 & 1 & 1 & 1 & 1 & 1 & 1 & 1 & 1 & 1 & 1 \end{bmatrix}$$

with the region in the vicinity of maxillary plane, started from Superior Incisor, determines the best matched clusters for maxillary and occlusal planes, respectively.

In pediatric skull cephalograms, detection of the planes is relatively difficult. In order to find the occlusal plane both maxillary and mandible need to be identified. It will be even more difficult if the Superior Incisor is not detected. By imposing constraints to the size of search area, in this case, a number of clusters belonging to the occlusal plane and/or the planes between old and new generation of teeth will be detected. Maxillary and mandibular location information is then exploited in detection of dominant points for the occlusal plane; the occlusal plane must have reasonable distance (almost equal) from both maxillary and mandibular planes.

After all classes are determined based on the above procedure, the following implications have to be fuzzified [4]:

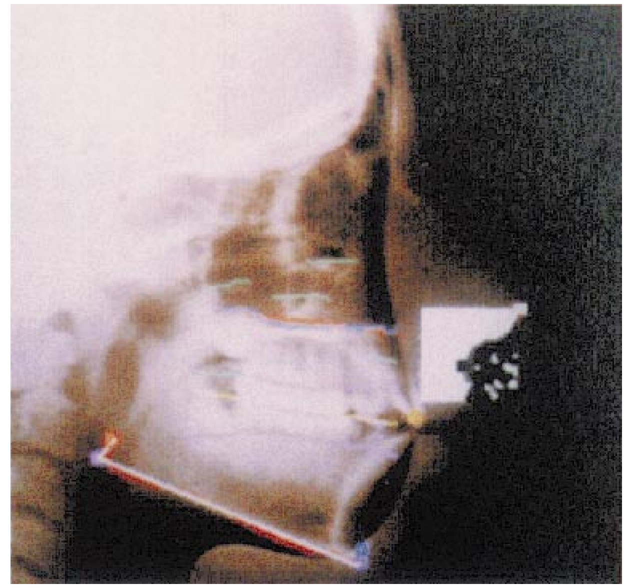

Fig. 6. Bilevel profile of the subnasal region.

1. the line (Occlusal plane) must be "long";
2. the distance between the line and Superior Incisor is "minimum";
3. the angle of the planes with respect to the horizon is "less than 45°".

The fuzzification process requires definition of membership functions for each linguistic variable. The empirical membership functions for *long* and *less than 45°* are depicted in Fig. 8.

4.5. Mandibular plane, Menton and Gonion

Menton is on the right end of lower jaw border line (mandibular plane) and gonion is on its left end. To find Menton a search is carried out column by column from the right side in a window of size 120×120 from the right

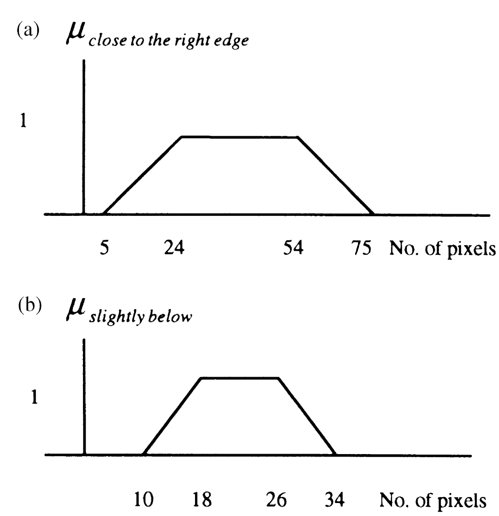

Fig. 7. Membership functions for: (a) close to the right; and (b) slightly below.

bottom corner over the hard-tissue-enhanced bilevelized image. As soon as a non-zero point is detected the search terminates for current line and starts for the next vertical line. Each detected point is allocated to the class whose representative is the spatial mean over a region of radius 25. The dominant cluster will be the one with the largest number of members and closer to the lower-right corner.

To find the exact location of Menton, a 15×15 template defined as

$$N_7 = \begin{bmatrix} 1 & 1 & 1 & 1 & 1 & 10 & 10 & 10 & 10 & -1 & -1 & -1 & -1 & -1 & -1 \\ 1 & 1 & 1 & 1 & 1 & 10 & 10 & 10 & 10 & -1 & -1 & -1 & -1 & -1 & -1 \\ 1 & 1 & 1 & 1 & 1 & 10 & 10 & 10 & 10 & -1 & -1 & -1 & -1 & -1 & -1 \\ 1 & 1 & 1 & 1 & 1 & 10 & 10 & 10 & 10 & -1 & -1 & -1 & -1 & -1 & -1 \\ 1 & 1 & 1 & 1 & 1 & 10 & 10 & 10 & 10 & -1 & -1 & -1 & -1 & -1 & -1 \\ 10 & 10 & 10 & 10 & 10 & 10 & 10 & 10 & 10 & -1 & -1 & -1 & -1 & -1 & -1 \\ 10 & 10 & 10 & 10 & 10 & 10 & 10 & 10 & 10 & -1 & -1 & -1 & -1 & -1 & -1 \\ 10 & 10 & 10 & 10 & 10 & 10 & 10 & 10 & 10 & -1 & -1 & -1 & -1 & -1 & -1 \\ 10 & 10 & 10 & 10 & 10 & 10 & 10 & 10 & 10 & -1 & -1 & -1 & -1 & -1 & -1 \\ 10 & 10 & 10 & 10 & 10 & 10 & 10 & 10 & 10 & -1 & -1 & -1 & -1 & -1 & -1 \\ -1 & -1 & -1 & -1 & -1 & -1 & -1 & -1 & -1 & -1 & -1 & -1 & -1 & -1 & -1 \\ -1 & -1 & -1 & -1 & -1 & -1 & -1 & -1 & -1 & -1 & -1 & -1 & -1 & -1 & -1 \\ -1 & -1 & -1 & -1 & -1 & -1 & -1 & -1 & -1 & -1 & -1 & -1 & -1 & -1 & -1 \\ -1 & -1 & -1 & -1 & -1 & -1 & -1 & -1 & -1 & -1 & -1 & -1 & -1 & -1 & -1 \\ -1 & -1 & -1 & -1 & -1 & -1 & -1 & -1 & -1 & -1 & -1 & -1 & -1 & -1 & -1 \end{bmatrix}$$

and a 30×30 sub-block of image in the cluster neighborhood are cross-correlated. The statistical correlation function is defined as

$$R_i(j) = \frac{\sum_{l=-7}^{7} \sum_{m=-7}^{7} (N_7(l+7, m+7) - N_m)(X(i+l, j+m) - X_m^{i,j})}{\sqrt{\sum_{l=0}^{14} \sum_{m=0}^{14} (N_7(l,m) - N_m)^2 \sum_{l=-7}^{7} \sum_{m=-7}^{7} (X(i+l, j+m) - X_m^{i,j})^2}} \quad (5)$$

where $X_m^{i,j}$ corresponds to the mean of grey values of the pixels lying on the ith column of the image sub-block within the window centered at point (i, j). The maximum of R corresponds to Menton.

To find the mandibular plane, the strategy in Section 3 is followed to detect the edge points. Then by using LSF criterion, the best-fitted straight line to the points is determined. This line is the best approximation to the mandibular plane. The mandibular, maxillary and occlusal planes are almost parallel.

Gonion is not however, necessarily located on the above approximated mandible line. To locate Gonion, a search similar to the one used for detection of Menton is conducted using a similar but opposite in left-right direction template. As Gonion is located on the margin and one corner of hard tissue, the number of clusters is limited. The dominant cluster will be located close to the left end of the mandible. In this cluster the member with the lowest distance to the mandibular plane is chosen as Gonion.

The *AP man* point may also be exactly identified by extrapolation of lower jaw plane to the right.

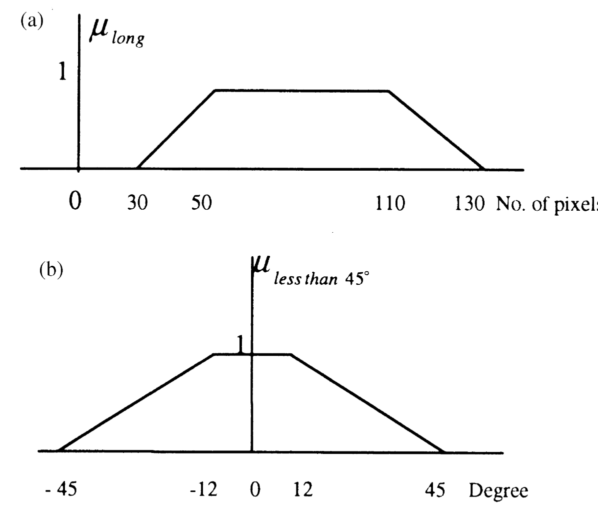

Fig. 8. The membership functions for: (a) long; and (b) less than 45°.

4.6. Subspinal point A

Point A is located in the deepest point to the left on the margin of hard and soft tissue above Superior Incisor between the maxillary and occlusal planes. A search is carried out in a region of 60×70 of hard-tissue-enhanced image both sides above Superior Incisor. A 3×3 template, N_8, as defined as

$$N_8 = \begin{bmatrix} 1 & 0 & -1 \\ 1 & 0 & -1 \\ 1 & 0 & -1 \end{bmatrix}$$

is utilized to detect the margin. The margin points may be the local maxima of cross-correlation of N_8 and the image within a window of radius 5. The extreme left point of this margin is easily identified by scanning a region, including all detected points, vertically. Due to the noisy nature of image data the desired point will be the one with the highest number of neighbors in the vertical direction. Each detected point, which has a value more than the average plus the variance of the cross-correlation function, will belong to a cluster.

4.7. Supramental point B

Point B is normally at the left side and between the Superior Incisor and Menton. The search and template matching steps are similar to those of point A. The search area is

inside a rectangular region ended by Superior Incisor on the upper side and by Menton on the lower side.

4.8. Sella Turcica

Sella is the most important lateral skull feature as a reference point for detection of occlusal abnormalities. The landmark S is in the centre of this curve-shape feature. To locate S, Sella Turcica has to be detected. Although Sella usually appears to have a grey level higher than its vicinity region, accurate identification of Sella suffers from its variable size, variable shape, rotation and displacement. Various methods such as application of Fourier descriptors and Artificial Neural networks (ANN) have been investigated by some researchers [3]. However, to overcome all the above problems a criterion based on structural and statistical pattern recognition has been developed. The technique exploits the above concepts together with primary geometrical information in order to detect the exact shape and location of Sella.

Sella is normally located in the upper left quarter of the skull image. Moreover, Sella is connected, from the right side, to the lower margin of the forehead. The extrapolation of the forehead to the left together with the the Sella curve provides a closed loop. The point S is located in the center of this loop and the point called Mid point of entrance to Sella, is located above S almost on the extension of the forehead line.

To detect Sella, the upper-left quarter of the image is taken into consideration. The edges are enhanced and the noise is reduced using a two-dimensional band-pass Gaussian filter ($\mu = 40$, $\sigma^2 = 20$). The forehead edge is detected by applying an edge tracing and linking algorithm. The best fit straight line gives an approximation to the forehead margin in this quarter. The line is extrapolated to the left enough to enclose entrance to the Sella. Then a search is carried out to find the maximum correlation between appropriate 10×10 templates and the image sub-block in scanning fashion. N_9 is used to detect horizontal segments (—), N_{10} to detect vertical segments (|), N_{11} to detect left-up 90° angles (⌟) and N_{12} to extract right-down 90° corners (⌜). These templates are defined as

$$N_9 = \begin{bmatrix} 0 & 0 & 0 & 0 & 0 & 0 & 0 & 0 & 0 & 0 \\ 0 & 0 & 0 & 0 & 0 & 0 & 0 & 0 & 0 & 0 \\ 0 & 0 & 0 & 0 & 0 & 0 & 0 & 0 & 0 & 0 \\ 0 & 0 & 0 & 0 & 0 & 0 & 0 & 0 & 0 & 0 \\ 255 & 255 & 255 & 255 & 255 & 255 & 255 & 255 & 255 & 255 \\ 255 & 255 & 255 & 255 & 255 & 255 & 255 & 255 & 255 & 255 \\ 0 & 0 & 0 & 0 & 0 & 0 & 0 & 0 & 0 & 0 \\ 0 & 0 & 0 & 0 & 0 & 0 & 0 & 0 & 0 & 0 \\ 0 & 0 & 0 & 0 & 0 & 0 & 0 & 0 & 0 & 0 \\ 0 & 0 & 0 & 0 & 0 & 0 & 0 & 0 & 0 & 0 \end{bmatrix}$$

$$N_{10} = \begin{bmatrix} 0 & 0 & 0 & 0 & 250 & 250 & 0 & 0 & 0 & 0 \\ 0 & 0 & 0 & 0 & 250 & 250 & 0 & 0 & 0 & 0 \\ 0 & 0 & 0 & 0 & 250 & 250 & 0 & 0 & 0 & 0 \\ 0 & 0 & 0 & 0 & 250 & 250 & 0 & 0 & 0 & 0 \\ 0 & 0 & 0 & 0 & 250 & 250 & 0 & 0 & 0 & 0 \\ 0 & 0 & 0 & 0 & 250 & 250 & 0 & 0 & 0 & 0 \\ 0 & 0 & 0 & 0 & 250 & 250 & 0 & 0 & 0 & 0 \\ 0 & 0 & 0 & 0 & 250 & 250 & 0 & 0 & 0 & 0 \\ 0 & 0 & 0 & 0 & 250 & 250 & 0 & 0 & 0 & 0 \\ 0 & 0 & 0 & 0 & 250 & 250 & 0 & 0 & 0 & 0 \end{bmatrix}$$

$$N_{11} = \begin{bmatrix} 0 & 0 & 0 & 0 & 255 & 255 & 0 & 0 & 0 & 0 \\ 0 & 0 & 0 & 0 & 255 & 255 & 0 & 0 & 0 & 0 \\ 0 & 0 & 0 & 0 & 255 & 255 & 0 & 0 & 0 & 0 \\ 0 & 0 & 0 & 0 & 255 & 255 & 0 & 0 & 0 & 0 \\ 255 & 255 & 255 & 255 & 255 & 255 & 0 & 0 & 0 & 0 \\ 255 & 255 & 255 & 255 & 255 & 0 & 0 & 0 & 0 & 0 \\ 0 & 0 & 0 & 0 & 0 & 0 & 0 & 0 & 0 & 0 \\ 0 & 0 & 0 & 0 & 0 & 0 & 0 & 0 & 0 & 0 \\ 0 & 0 & 0 & 0 & 0 & 0 & 0 & 0 & 0 & 0 \\ 0 & 0 & 0 & 0 & 0 & 0 & 0 & 0 & 0 & 0 \end{bmatrix}$$

$$N_{12} = \begin{bmatrix} 0 & 0 & 0 & 0 & 0 & 0 & 0 & 0 & 0 & 0 \\ 0 & 0 & 0 & 0 & 0 & 0 & 0 & 0 & 0 & 0 \\ 0 & 0 & 0 & 0 & 0 & 0 & 0 & 0 & 0 & 0 \\ 0 & 0 & 0 & 0 & 0 & 0 & 0 & 0 & 0 & 0 \\ 0 & 0 & 0 & 0 & 0 & 255 & 255 & 255 & 255 & 255 \\ 0 & 0 & 0 & 0 & 255 & 255 & 255 & 255 & 255 & 255 \\ 0 & 0 & 0 & 0 & 255 & 255 & 0 & 0 & 0 & 0 \\ 0 & 0 & 0 & 0 & 255 & 255 & 0 & 0 & 0 & 0 \\ 0 & 0 & 0 & 0 & 255 & 255 & 0 & 0 & 0 & 0 \\ 0 & 0 & 0 & 0 & 255 & 255 & 0 & 0 & 0 & 0 \end{bmatrix}$$

Proper combination of these templates provides a reasonable estimation of Sella shape. Maximum correlation values between the templates and the image sub-blocks inside the search area, denotes the corresponding segment whose centre coincides with the centre of the template. The correlation function, Q, using all three types of templates is calculated similarly to the procedure for calculation of R in Section 4.5. Mean, variance and absolute maximum of Q are calculated. A local maxima of Q_1 (for N_9) subject to meeting the following conditions is added to our

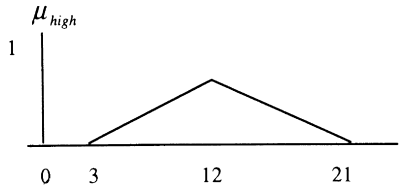

Fig. 9. The membership function for the linguistic parameter high.

classification system.

$$\begin{cases} (Q_{1\max} - Q_{1\text{mean}}) \times \frac{3}{4} < Q_{1c} \\ Q_{1\max} > 0.3 \end{cases} \quad (6)$$

where Q_{1c} denotes the centre of the window. Similar conditions are imposed on the functions Q_2, Q_3 and Q_4 corresponding to N_{10}, N_{11} and N_{12}, respectively. A number of candidates may be appointed for each segment. Upon structural and relative geometrical parameters a boundary portion including a number of the above segments will be recognized by implementing a FL-based reasoning system. For the winning cluster:

1. the segments ⌜ are above the segments — and ⌟ but "not very far" from them;
2. the segments | are above-left and above-right of —;
3. the geometrical distance between the two segments — and ⌟ is "small";
4. spatial means of —, |, ⌟ and ⌜ provide angles "close to 90°";
5. all the segments are located below the extended forehead margin.

4.9. Nasion

Nasion is located in front and to the right hand side of Sella. It is also the deepest point on the margin of soft and hard tissues. Priori information about Sella is exploited in detection of Nasion. The search area is located within an angle of -20 to $+20$ with respect to the horizontal line started from Sella to the right. The region is filtered, in order to get rid of high frequency noise, using a lowpass, fifth-order two-dimensional Butterworth filter [8] having a cutoff spatial frequency of $f_c = 25$. Then the smooth image is bilevelised. The coordinates of the points on the margin are saved in a one-dimensional array (x as a function of y). The array is smoothed using averaging over each of the five elements. The image is then cross-correlated with the template N_{13} defined as

$$N_{13} = \begin{bmatrix} 1 & 2 & -2 & -1 \\ 1 & 2 & -2 & -1 \\ 1 & 2 & -2 & -1 \\ 1 & 2 & -2 & -1 \end{bmatrix}$$

Assuming the correlation matrix to be ρ_n, the window centre

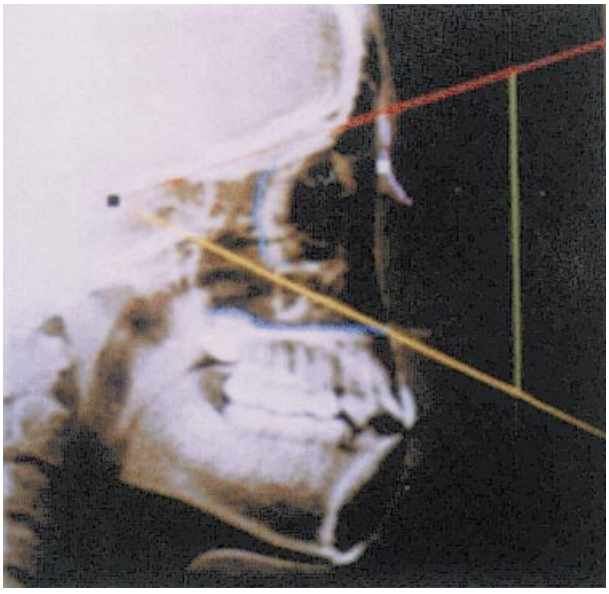

Fig. 10. The search area, the curve shape segment and Nasion.

points which are local maxima and satisfy the conditions

$$\rho_{wc} > \mu_\rho + 0.7\sigma_\rho^2 \quad (7)$$

(where ρ_{wc} denotes the window centre, μ_ρ and σ_ρ^2 are mean and variance of ρ, respectively) are considered as cluster members. Among the classes those belonging to the line segments of at least five-element length are selected. The segment including Nasion is then obtained by the following fuzzy criteria:

1. the number of elements (points) is "high";
2. it has maximum curvature.

The fuzzy membership function for high is depicted in Fig. 9. To find the degree of curvature function $K(y)$ proportional to the second-order derivative, $g''(y)$, is calculated by using the following equations.

If $x = g(y)$ for the margin line, then

$$K(y) = \frac{|g''(y)|}{[1 + g''(y)^2]^{3/2}} \quad (8)$$

where

$$g''(y) = \frac{d^2 g(y)}{dy^2} \quad (9)$$

The minimum or beginning of an increasing point (in the case where the minimum does not exist) is considered as Nasion. Fig. 10 illustrates the searching area, curve shape segments and Nasion.

4.10. Analysis of final results by FL

Although the applied method for detection of each landmark has been highly dependent on the geometrical relationship of the points, a global FL-based reasoning system may be implemented to further justify the results. This

Fig. 11. The final extracted landmarks.

includes empirical definition of membership functions for the geometrical parameters such as link and angle sizes. Any selected point beyond the approximated range is discarded and the search for the landmark is repeated.

In all cases, the decision is made based on the defuzzified information. The defuzzification process follows the method called Centre of Area (COA) for which the defuzzified parameter, c, is related to the output membership function, μ_c, via the following relationship [4].

$$F^1(c) = \frac{\int_w w\mu_c(w)\,\mathrm{d}w}{\int_w \mu_c(w)\,\mathrm{d}w} \tag{10}$$

5. Conclusions

The final set of extracted landmarks are depicted in Fig. 11. The majority of the features are extracted with 100% accuracy from the cephalograms of about 20 adults and 5 children. In comparison with previous methods for which the accuracy of the results has been reported [3], the proposed criterion in this paper achieves higher accuracy in locating the landmarks. In the application of approximate reasoning in exploitation of relative landmark locations, data statistics and image structure, maximum informative clinical data has been taken into consideration. Thus the efficiency of the system and the accuracy of the results are remarkably enhanced. Definition of a proper template to match each specific feature requires a priori knowledge about the landmark. This can be easily obtained by first glance and it is not dependent on any specific cephalogram.

The outcome of the process may be used for clinical diagnosis and design of an expert system [10] as well as medical and dental education.

References

1 J.R.E. Mills, Principles and Practice of Orthodontics, Churchill Livingstone, London, 1987.
[2] T. Rakosi, An Atlas and Manual of Cephalometric Radiography, Wolf Medical Publication, England, 1982.
[3] J. Cardillo, An image processing system for locating craniofacial landmarks, IEEE Trans. Med. Imaging 13 (2) (1994) 275–290.
[4] R.R. Yager, D.P. Filev, Essentials of Fuzzy Modeling and Control, Wiley, New York, 1994.
[5] M.A. Blommer, G.H. Waketield, The side information median filter for sequence reconstruction, IEEE Trans. Signal Processing 43 (5) (1995) 1033–1035.
[6] D. Hudson, M.E. Cohen, Fuzzy logic in medical expert systems, IEEE Engng. Med. Biology 5 (6) (1994) 693–698.
[7] H. Avi-Itzhak, et al., Subclass pattern recognition: A maximum correlation approach, IEEE Trans. Pattern Anal. Machine Intelligence 17 (4) (1995) 418–428.
[8] R.C. Gonzales, M. Woods, Digital Image Processing, 3, Addison-Wesley, Reading, MA, 1992.
[9] J.B. Zimmerman, et al., Evaluation of effectiveness of adaptive histogram equalization for contrast enhancement, IEEE Trans. Med. Imaging 7 (4) (1988) 304–312.
[10] N. Mackin, J.H. Sims-Williams, Artificial intelligence in dental surgery: An orthodontic expert system. A dental tool for tomorrow, J. Orthodontics October (1991) 341–343.